

# Slow-light-induced interference with stacked optical precursors for square input pulses

Heejeong Jeong<sup>1,3</sup> and Shengwang Du<sup>2,4</sup>

<sup>1</sup>*Samsung Electronics Co., Ltd., Suwon, Gyeonggi 443-742, Korea*

<sup>2</sup>*Department of Physics, The Hong Kong University of Science and Technology, Clear Water Bay, Kowloon, Hong Kong, China*

<sup>3</sup>*jhj413@gmail.com*

<sup>4</sup>*dusw@ust.hk*

Received July 23, 2009; revised November 29, 2009; accepted December 1, 2009; posted December 16, 2009 (Doc. ID 114444); published January 11, 2010

We theoretically study the stacked optical transients generated from a series of square pulses passing through a cold atomic ensemble. Using the hybrid analysis and fast Fourier transform, we identify the stacked coherent transients [Europhys. Lett. **4**, 47 (1987)] as optical precursors. With slow-light and electromagnetically induced transparency, we obtain nearly 700% transmitted intensity at the transient spikes resulting from the interference between the delayed main field and the stacked optical precursors.

© 2010 Optical Society of America  
OCIS codes: 070.7345, 270.1670.

Optical precursors [1,2] in anomalously dispersive media, analogous to coherent transients [3,4], recently have been of great interest owing to their non-decaying properties [5] as well as their instantaneous speed of light in vacuum  $c$ . Analogy between optical precursors and coherent transients was noticed by Varoquaux *et al.* [6] by using time-domain analysis. However, the analogy was not accepted by both communities of optical precursors [2] and coherent transients [3,4], because the conventional concept of optical precursors was established based on strongly dispersive far-off resonance condition [1,2].

Recent experimental study of optical precursors in cold atoms [5] has triggered unifying both concepts [7,8] to include phenomena such as resonantly filtered gamma-ray [9] and small-area ( $0\pi$ ) pulses [10]. Motivated by the observation of precursory spikes at the leading edge of biphoton correlation with electromagnetically induced transparency (EIT) [11,12], the classical step-on pulse transmission in EIT medium has been studied theoretically [13,14]. Most recently, observation of optical precursors at both rising and falling edges of a square pulse passing through an EIT system has been reported [15]. Combining EIT and optical precursors makes it possible to control the delay between precursors and main signal for the application of active optical devices.

In coherent transients, one of the interesting effects is the stacking of the coherent transients by Segard *et al.* [4]. About 300% output with respect to the input intensity was achieved by sending a series of square pulses through an optically thick single Lorentz-line medium. Stacking of coherent transients at edges results in output peaks larger than the input intensity [4]. In their early works [4,16], however, the possibility of optical precursors had been excluded until recently [14].

In this Letter, we first identify, in a two-level system, Segard's coherent stacks [4] as the stack of Sommerfeld–Brillouin precursors at the rising and falling edges of square pulses using the asymptotic

saddle-point method. In an optically thick EIT medium, we take the hybrid method to describe the relevant main signal and precursors [13]. The hybrid method for a Heaviside step-on modulated incident pulse  $\Theta(t)$  is modified to describe a step-off modulated pulse  $\Theta(-t)$ . The result shows how the delayed main signal (slow light) interferes with the transients (precursors) when the steady external laser beam is suddenly turned off. The transient peak intensity turns out to be 180% with respect to the input intensity. The schematic illustration of pulse propagation is shown in Fig. 1, where the on-resonance coupling laser between the transition  $|2\rangle \leftrightarrow |3\rangle$  renders a narrow transparency window on the pulse carrier frequency  $\omega_p$  that is on resonance of the transition  $|1\rangle \rightarrow |3\rangle$ ,  $\omega_0$ . Finally, we extend the single-square pulse to multisquare pulses and obtain 700% output peak transmission in the EIT medium.

The linear susceptibility of the EIT medium is given in Eq. (1) of [13] as

$$\chi(\omega) = \frac{c\alpha_0}{\omega_0} \frac{4(\Delta + i\delta_{12})\delta}{\Omega_c^2 - 4(\Delta + i\delta_{12})(\Delta + i\delta)}, \quad (1)$$

where  $\Delta = \omega - \omega_0$  is the probe laser angular frequency detuning,  $\alpha_0 z = 62$  is the optical depth,  $\delta = 2\pi$

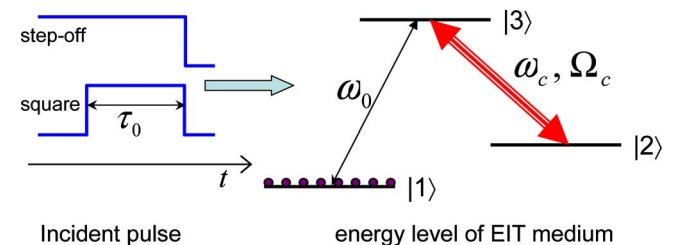


Fig. 1. (Color online) Illustration of a step-off or square pulse propagation through an EIT medium. The carrier frequency of the incident pulse  $\omega_p = \omega_0$  is on resonance of the transition  $|1\rangle \rightarrow |3\rangle$ . The coupling laser ( $\omega_c$ ) is on resonance of the transition  $|2\rangle \rightarrow |3\rangle$  with a Rabi frequency of  $\Omega_c$ .

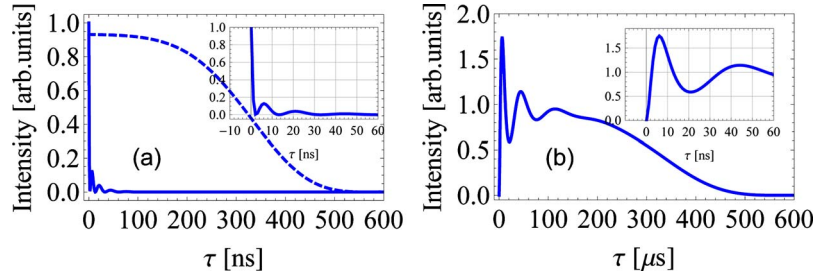


Fig. 2. (Color online) Normalized intensities of (a) total precursors (solid curve) and the main signal (dashed curve) and (b) total intensity at the falling edge of a step-off input pulse.

$\times 3$  MHz is half of the natural linewidth,  $\delta_{12} = 0.005\delta$  is the dephasing rate between the two ground levels, and  $\Omega_c = 4.20\delta$  is the coupling laser Rabi frequency. The integral form of the transmitted pulse is given in Eq. (2) of [13]. The initial weak probe pulse is given as  $E_{\pm}(0, t) = E_0\Theta(\pm t)e^{-i\omega_p t}$  where “+” stands for the step-on pulse with a rising edge and “-” stands for the step-off pulse. Their frequency spectrums is  $E_{\pm}(0, \Delta)/E_0 = \pm i/\Delta + \pi\delta(\Delta)$ . This allows us to directly apply the hybrid-asymptotic analysis in [13] to obtain the precursors for the step-off pulse by multiplying a factor of  $-1$  to that for the step-on pulse. Thus the total Sommerfeld–Brillouin precursor for the step pulse can be obtained from Eqs. (5) and (6) of [13], and approximated as a Bessel function [15,17] explaining oscillatory patterns in insets of Figs. 2 and 3:

$$E_{SB_{\pm}}(z, t) \approx \pm E_0 J_0(\sqrt{2\alpha_0 z \delta \tau}) \Theta(\tau) e^{-\delta \tau} e^{i(k_0 z - \omega_0 \tau)}, \quad (2)$$

where  $\tau = t - z/c$  and  $k_0 = \omega_0/c$ .

To avoid the singularity of  $E_-(0, \Delta)$  at  $\Delta = 0$ , we express the main field  $E_{M-}(z, t)$  for the step-off pulse as a convolution of the input pulse and the Green function  $G_{EIT}(z, t)$  of the EIT window  $[\omega_0 - \Delta_e, \omega_0 + \Delta_e]$  [13]:

$$E_{M-}(z, t) = E_0 \int_{-\infty}^0 G_{EIT}(z, t - \tau) d\tau, \quad (3)$$

where  $\Delta_e \leq \Omega_c/2$  is the full width of the EIT window. With EIT slow-light effect, the main field is delayed and  $E_{M-}(z, t)$  can be approximated as a constant field within the time when the precursors occur [15].

The normalized intensities of total precursors  $|E_{SB-}(z, t)|^2/E_0^2$  and the main signal  $|E_{M-}(z, t)|^2/E_0^2$  are shown in Fig. 2(a). Figure 2(b) shows the total intensity  $|E_-(z, t)|^2/E_0^2 = |E_{M-}(z, t) + E_{SB-}(z, t)|^2/E_0^2$ . The falling edge of the main field is delayed by about 300 ns owing to the EIT slow-light effect. The interference between the main and precursor fields leads to damped oscillation with a normalized peak intensity of 180% and a decay time of  $1/\delta = 52$  ns.

Transmission of a square input pulse  $E_{sq}(0, t) = E_0[\Theta(t) - \Theta(t - \tau_0)]e^{-i\omega_p t}$ , is given by  $E_{sq}(z, t) = E_{SB_{sq}}(z, t) + E_{M_{sq}}(z, t)$ , where  $E_{SB_{sq}}(z, t) = E_{SB_+}(z, t) - E_{SB_+}(z, t - \tau_0)$  and  $E_{M_{sq}}(z, t) = E_{M_+}(z, t) - E_{M_+}(z, t - \tau_0)$ . Figure 3 shows the normalized total transmission intensity compared with fast Fourier transform (FFT) simulations. The oscillatory pattern at the falling edge is identical to the Bessel function oscillatory pattern that appeared in a step-off pulse [Fig. 2(b)].

The slow-light induced interference at the falling edge is identical to the case for the step-off input pulse.

By using Eqs. (2) and (3), we first evaluate the maximum value of the stacked output for the input pulse  $E(0, t)/E_0 = \Theta(t) + \Theta(t - \tau_0) + \sum_{i=1}^{i=5} (-1)^i \Theta(t - \tau_0 + t_i)$ , where  $t_i = j_{1,i}^2 / (2\alpha_0 z \delta)$  and  $j_{1,i}$  is the  $i$ th zero of  $J_1(x)$  by considering the oscillatory pattern of precursors as originally discussed in [4]:

$$E_{SB_{stack}}(z, t) = E_{SB_+}(z, t) + E_{SB_+}(z, t - \tau_0) + \sum_{i=1}^{i=5} (-1)^i E_{SB_+}(z, t - \tau_0 + t_i), \quad (4)$$

$$E_{M_{stack}}(z, t) = E_0 \sum_{k=1}^2 \int_{\tau_0 - t_{2k-1}}^{\tau_0 - t_{2k}} G_{EIT}(z, t - \tau) d\tau + E_0 \left( \int_0^{\tau_0 - t_5} + \int_{\tau_0}^{\infty} \right) G_{EIT}(z, t - \tau) d\tau, \quad (5)$$

$$E_{stack}(z, t) = E_{SB_{stack}}(z, t) + E_{M_{stack}}(z, t). \quad (6)$$

We note that, in the EIT medium, the maximum intensity from stacked coherence occurs at the step-on edge  $t = \tau_0$  where the precursor is in phase with the delayed main field. For comparison, we show the

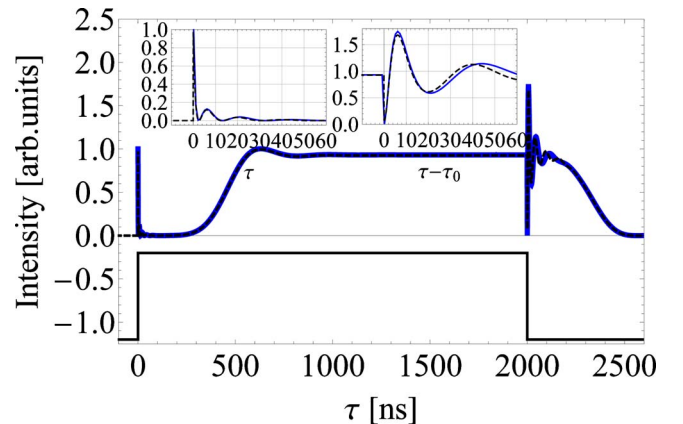


Fig. 3. (Color online) Normalized total intensities composed of optical precursors and delayed main signal in an EIT medium. Input square pulse  $E(0, t)$  is given as a solid line (shifted by  $-1.2$ ). Hybrid analysis [Eqs. (2) and (3), solid curves (blue online)] is compared with FFT (dashed curves).

stacked optical transient responses from both two-level and EIT systems in Fig. 4. As shown in Fig. 4(a), a peak transmission larger than unity (300%) is possible in the two-level system. In the EIT case, the constructive interference between the transient (300%) and delayed main field (93%) leads to a 700% intensity peak. The solid curves (blue online), obtained using the hybrid-asymptotic method [Eqs. (4)–(6)], display nearly identical features as that from FFT except for slightly different peak values resulting from the approximation of the hybrid analysis. Therefore, we identify that the stacked transients [4] are indeed an interference of optical precursors from different rising and falling edges. The dashed curves are obtained using FFT with a time resolution of 50 ps. Owing to the nature of FFT process, the 50 ps time resolution simulates a finite rise and fall time of 50 ps, and thus a bandwidth of 20 GHz that is commercially available. For the parameters given in this Letter, the optical transients generated from the square pulses with 50 ps rise (fall) time have been very close to that from ideal square pulses, because there is no significant difference as we reduce the rise

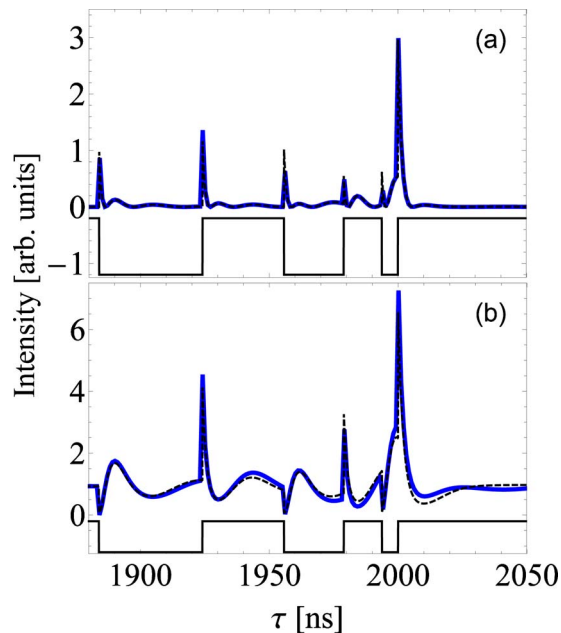


Fig. 4. (Color online) Normalized total intensities composed of a stack of optical precursors and delayed main signal for the case of (a) two-level ( $\Omega_c=0$ ) and (b) EIT medium ( $\Omega_c=4.2\delta$ ). The series of square pulses as input  $E(0,t)$  is given as a solid line (shifted by  $-1.2$ ). The hybrid analysis [Eqs. (4)–(6), solid curves (blue online)] is compared with FFT (dashed curves).

time from 50 ps to 5 ps. In a real situation, pulse generator and electronics also give rise to finite bandwidth. Thus the theoretical prediction should be associated with the low-pass filter as used in [5].

We have studied optical precursors generated from step-on, step-off and square pulses in an EIT system. The long-lived oscillatory tail over 100 ns time at the falling edge results from the interference between the precursor and main field. We further extend the single square input pulse to a series of square pulses and obtain about 700% peak transmission in the stacked optical transients. The agreement between FFT and hybrid-asymptotic methods confirms that the stack of coherent transients introduced by Segard *et al.* [4] is identified as the stack of optical precursors occurring at the rising and falling edges of square pulses.

The authors acknowledge the valuable suggestions from the reviewers.

## References

1. L. Brillouin, *Wave Propagation and Group Velocity* (Academic, 1960).
2. K. E. Oughstun and G. C. Sherman, *Electromagnetic Pulse Propagation in Causal Dielectrics* (Springer-Verlag, 1994).
3. M. D. Crisp, *Phys. Rev. A* **1**, 1604 (1970).
4. B. Segard, J. Zemmouri, and B. Macke, *Europhys. Lett.* **4**, 47 (1987).
5. H. Jeong, A. M. C. Dawes, and D. J. Gauthier, *Phys. Rev. Lett.* **96**, 143901 (2006).
6. E. Varoquaux, G. A. Williams, and O. Avenel, *Phys. Rev. B* **34**, 7617 (1986).
7. H. Jeong and U. L. Österberg, *J. Opt. Soc. Am. B* **25**, B1 (2008).
8. H. Jeong and U. L. Österberg, *Phys. Rev. A* **77**, 021803(R) (2008).
9. F. J. Lynch, R. E. Holland, and M. Hamermesh, *Phys. Rev.* **120**, 513 (1960).
10. J. E. Rothenberg, D. Grischkowsky, and A. C. Balant, *Phys. Rev. Lett.* **53**, 552 (1984).
11. S. Du, P. Kolchin, C. Belthangady, G. Y. Yin, and S. E. Harris, *Phys. Rev. Lett.* **100**, 183603 (2008).
12. S. Du, C. Belthangady, P. Kolchin, G. Y. Yin, and S. E. Harris, *Opt. Lett.* **33**, 2149 (2008).
13. H. Jeong and S. Du, *Phys. Rev. A* **79**, 011802(R) (2009).
14. B. Macke and B. Segard, *Phys. Rev. A* **80**, 011803(R) (2009).
15. D. Wei, J. F. Chen, M. M. T. Loy, G. K. L. Wong, and S. Du, *Phys. Rev. Lett.* **103**, 093602 (2009).
16. B. Macke and B. Segard, *Phys. Rev. A* **73**, 043802 (2006).
17. W. R. LeFew, S. Venakides, and D. J. Gauthier, *Phys. Rev. A* **79**, 063842 (2009).